UNIVERSITY OF AMSTERDAM

UvA-DARE (Digital Academic Repository)

Control over few-photon pulses by a time-periodic modulation of the photon emitter coupling

Pletyukhov, M.; Pedersen, K.G.L.; Gritsev, V.

DOI
10.1103/PhysRevA.95.043814

Publication date
2017

Document Version
Final published version

Published in
Physical Review A

Link to publication

Citation for published version (APA):
Pletyukhov, M., Pedersen, K. G. L., & Gritsev, V. (2017). Control over few-photon pulses by a time-periodic modulation of the photon emitter coupling. *Physical Review A*, *95*(4), Article 043814. https://doi.org/10.1103/PhysRevA.95.043814

General rights
It is not permitted to download or to forward/distribute the text or part of it without the consent of the author(s) and/or copyright holder(s), other than for strictly personal, individual use, unless the work is under an open content license (like Creative Commons).

Disclaimer/Complaints regulations
If you believe that digital publication of certain material infringes any of your rights or (privacy) interests, please let the Library know, stating your reasons. In case of a legitimate complaint, the Library will make the material inaccessible and/or remove it from the website. Please Ask the Library: https://uba.uva.nl/en/contact, or a letter to: Library of the University of Amsterdam, Secretariat, Singel 425, 1012 WP Amsterdam, The Netherlands. You will be contacted as soon as possible.

UvA-DARE is a service provided by the library of the University of Amsterdam (https://dare.uva.nl)

Download date:18 Oct 2025

Control over few-photon pulses by a time-periodic modulation of the photon emitter coupling

Mikhail Pletyukhov,[1] Kim G. L. Pedersen,[1] and Vladimir Gritsev[2]

[1]*Institute for Theory of Statistical Physics and JARA—Fundamentals of Future Information Technology, RWTH Aachen University, 52056 Aachen, Germany*

[2]*Institute for Theoretical Physics, Universiteit van Amsterdam, Science Park 904, Postbus 94485, 1098 XH Amsterdam, The Netherlands*

(Received 17 March 2016; published 11 April 2017)

We develop a Floquet scattering formalism for the description of quasistationary states of microwave photons in a one-dimensional waveguide interacting with a nonlinear cavity by means of a periodically modulated coupling. This model is inspired by the recent progress in engineering of tunable coupling schemes with superconducting qubits. We argue that our model can realize the quantum analog of an optical chopper. We find strong periodic modulations of the transmission and reflection envelopes in the scattered few-photon pulses, including photon compression and blockade, as well as dramatic changes in statistics. Our theoretical analysis allows us to explain these nontrivial phenomena as arising from nonadiabatic memory effects.

DOI: 10.1103/PhysRevA.95.043814

I. INTRODUCTION

Periodically driven quantum systems—or Floquet quantum systems as they are often called—may behave markedly different than their equilibrium counterparts, and it has been shown time and time again that this difference in behavior serves a whole range of potential applications.

In many-body quantum physics, intensive research has recognized that the periodic driving of quantum many-body system could create new synthetic phases of matter not accessible in equilibrium systems. This intuition, motivated by the classical example of the Kapitza pendulum [1], has been explored and confirmed in several contexts. In particular, some proposals predict the formation of topological phases [2–4] and artificial gauge systems [5–7], as well as localized nonthermal states in isolated many-body systems [8–12].

In quantum information protocols proposals for dynamical decoupling schemes [13–17] and their refinements [18–20] use periodic sequences of fast and strong symmetrizing pulses to reduce the parts of the system-bath interaction Hamiltonian which are sources of decoherence. Additionally, Floquet systems also naturally appear in digital quantum computation schemes [21]. In quantum transport various Floquet-driven quantum tunneling problems [22] are in the heart of physics described by effective two-level systems, quantum wells, and quantum open systems.

In this paper we seek to combine the possibilities offered by periodically driven quantum systems with the experimental flexibility available in quantum photonics as, e.g., realized in quantum optics or microwave quantum electrodynamics. At this point it is important to stress that we do not simply talk about the time dependence of, e.g., a classical laser field where the time dependence always trivially can be gauged away; instead we refer to quantum photonics systems where the time dependence manifests itself directly in the steady-state observables, i.e., such that they themselves become time dependent. Specifically we are interested in the long time behavior of the observables which can be captured by a suitably formulated version of scattering theory.

In classical optics the most common periodically driven instruments are optical choppers and shutters [23], famous perhaps for their application in the first nonastronomical speed-of-light measurements by Hippolyte Fizeau in 1849 [24], and used today, e.g., for speed or rotation measurements, light exposure control, and off-frequency noise filtering. The prototypical chopper uses a rotating wheel with holes that periodically block the incident light beam, with the added feature of being able to control the waveform of the chopped light through the hole-diameter to beam-width ratio [25].

One may imagine a quantum version of this instrument, with the light beam replaced by a weak coherent state of photons in a one-dimensional channel, and the rotating wheel by a single emitter that periodically couples to the channel. A key difference to the classical optical chopper is of course that a quantum chopper could potentially maintain a unitary evolution of the photons (when disregarding any losses). As we later discuss, such a quantum chopper could be used for single-photon pulse shaping [26], dynamical routing of single photons [27], and altering of the photon statistics [28,29].

Due to the nonlinear aspect of the emitter, a quantum chopper may also be able to modulate the statistics of the photons periodically in time. One may even speculate that the resulting periodically modulated signals may be used as input for other quantum optical instruments.

The experimental realization of a quantum chopper seems within the grasp of current nanophotonic technologies that allow tunable and controllable manipulation of the coupling between different photonic elements. Various tunable coupling schemes have already been proposed and implemented with superconducting qubits, essentially based on the tunability of the Josephson inductance [30–33]. Dynamic control has also been demonstrated using an external coupling element between two directly coupled phase and flux qubits [34–37], between a phase qubit and a lumped element resonator [38], and between a charge qubit and a coplanar waveguide cavity [39]. The latter scheme uses quantum interference to provide an intrinsic method to control the coupling. Recently a qubit architecture that incorporates fast tunable coupling and high coherence has been demonstrated, with dynamical tunability at nanosecond resolution [40].

 ©2017 American Physical Society

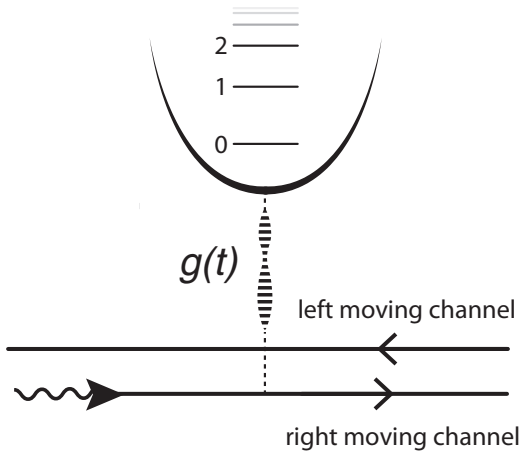

FIG. 1. Quantum chopper model consisting of a one-dimensional transmission line supporting two counterpropagating channels, and a cavity with a nonlinear spectrum. The two couple through a periodic coupling $g(t)$.

We model the proposed quantum analog of the chopper by the following Hamiltonian:

$$\begin{aligned} H(t) &= H_0 + V(t) \\ &= \int d\omega \hbar\omega (a_\omega^\dagger a_\omega + \tilde{a}_\omega^\dagger \tilde{a}_\omega) + \hbar\omega_c b^\dagger b + \frac{U}{2} b^{\dagger 2} b^2 \\ &\quad + \hbar g(t) \int d\omega \, (a_\omega^\dagger b + b^\dagger a_\omega). \end{aligned} \tag{1}$$

Here $a_\omega = (a_{r\omega} + a_{l\omega})/\sqrt{2}$ and $\tilde{a}_\omega = (a_{r\omega} - a_{l\omega})/\sqrt{2}$ describe the two waveguide fields expressed in terms of right- and left-moving modes, $g(t)$ is the coupling strength, and the emitter, described by the bosons $b, b^\dagger$, has been generalized to a nonlinear cavity characterized by a resonance frequency ω_c, and a nonlinearity U. An illustration of the model is also shown in Fig. 1.

In the following sections we first show how to solve the quasistationary dynamics of this system through a generalization of diagrammatic scattering theory to Floquet systems. Then we apply the Floquet scattering theory for describing open Floquet quantum systems explicitly in the few-photon limit. Various results for reflection, transmission, and statistics are then summarized. The method is general and can directly be applied to more intricate quantum systems.

II. FLOQUET SCATTERING FORMALISM

An extension of the scattering formalism for time-periodic Hamiltonians was originally proposed in Ref. [41] for the calculation of above-threshold-ionization spectra. Remarkably, it offered an effectively time-independent description of the quasistationary limit in terms of the Floquet states. Later, similar scattering approaches were developed for single-particle scattering [42,43], many-body scattering of noninteracting [44,45], and interacting [46] particles in driven systems.

Let us briefly review the basic ideas of scattering theory. Suppose that at time $t_0 \to -\infty$ we inject N photons into the transmission line while the cavity is empty. In second quantization, this incoming state is given by $|p\rangle \equiv |\{\omega_j\}\rangle|0\rangle_c = (\prod_{j=1}^N a_{\omega_j}^\dagger)|0\rangle|0\rangle_c$, where the vacuum state $|0\rangle$ of the transmission line is defined by $a_\omega|0\rangle = \tilde{a}_\omega|0\rangle = 0$, and $|l\rangle_c$ is the photon number state of the cavity, $b^\dagger b|l\rangle_c = l|l\rangle_c$. The energy of the incoming state equals $\varepsilon_p = \sum_{j=1}^N \omega_j$, where we have set $\hbar = 1$, as we will continue to do in the rest of this paper. After scattering, at time $t \to +\infty$, the cavity is empty again. Since the Hamiltonian (1) conserves a number of excitations, a scattering state $S|p\rangle$ also contains N photons. Here S is a scattering operator which emerges from a time evolution operator in the long time limit. In the case of the time-independent interaction V the energy ε_p of the input state is conserved in the following sense: matrix elements $S_{p'p} = \langle p'|S|p\rangle$ appear to be proportional to delta functions $\delta(\varepsilon_{p'} - \varepsilon_p)$, where $\varepsilon_{p'} = \sum_{j=1}^N \omega_j'$ is the energy of a state $|p'\rangle$. Moreover, $S_{p'p} = \delta_{p'p} - 2\pi i \delta(\varepsilon_{p'} - \varepsilon_p) T_{p'p}(\varepsilon_p)$, where $T_{p'p}(E)$ is the energy-dependent T operator containing all the information about scattering off the cavity. A systematic way of computing $T(E)$ has been developed in [47] for scatterers with an arbitrary level structure and transition matrix elements.

Following the ideas of [41] we now elaborate on the Floquet scattering formalism, particularly adapting it to problems of multiparticle scattering of (microwave) photons in one-dimensional waveguides interacting with (artificial) atoms. Our goal is to present a systematic way of computing the scattering operator S for a time-periodic interaction, $V(t) = V(t+T) = \sum_m V^{(m)} e^{-im\Omega t}$, with a fundamental frequency $\Omega = \frac{2\pi}{T}$, in the Floquet-extended Hilbert space, thereby generalizing the approach of Ref. [47] for time-independent couplings.

We start from an equation for the evolution operator in the interaction picture

$$i \frac{dU_{\rm int}(t,t_0)}{dt} = V_{\rm int}(t) U_{\rm int}(t,t_0), \tag{2}$$

where $V_{\rm int}(t) = e^{iH_0 t} V(t) e^{-iH_0 t}$. Taking the limit $t_0 \to -\infty$ we transform Eq. (2) into the integral form

$$U_{\rm int}(t) = \hat{1} - i \int_{-\infty}^{t} dt' e^{\eta t'} V_{\rm int}(t') U_{\rm int}(t'), \tag{3}$$

where an infinitesimal factor $\eta > 0$ is additionally introduced for convergence.

Next we define matrix elements $U_{p'p}(t) = \langle p'|U_{\rm int}(t)|p\rangle$ in the eigenbasis $\{|p\rangle\}$ of H_0, and express Eq. (3) in the matrix form

$$\begin{aligned} U_{p'p}(t) = \delta_{p'p} - i \int_{-\infty}^{t} dt' \sum_q \sum_m e^{i(\varepsilon_{p'} - \varepsilon_q - m\Omega - i\eta)t'} \\ \times V_{p'q}^{(m)} U_{qp}(t'). \end{aligned} \tag{4}$$

Being interested in a solution of this equation at times $t > 0$, satisfying the condition $\eta t \ll 1$, we look for it in the form

$$U_{p'p}(t) = \delta_{p'p} - \sum_{m'} \frac{e^{i(\varepsilon_{p'} - \varepsilon_p - m'\Omega)t}}{\varepsilon_{p'} - \varepsilon_p - m'\Omega - i\eta} \Theta_{p'p}^{(m')}, \tag{5}$$

where $\Theta^{(m')}_{p'p}$ are constant matrices. Plugging Eq. (5) into Eq. (4), we obtain

$$\Theta^{(m')}_{p'p} = V^{(m')}_{p'p} - \sum_q \sum_n \frac{V^{(m'-n)}_{p'q}\Theta^{(n)}_{qp}}{\varepsilon_q - \varepsilon_p - n\Omega - i\eta}, \tag{6}$$

from which we can establish the matrices $\Theta^{(m')}$.

At large times t we make in Eq. (5) the standard replacement $\frac{e^{i\omega t}}{\omega - i\eta} \to 2\pi i\delta(\omega)$, and thus obtain the scattering matrix

$$S_{p'p} = \delta_{p'p} - 2\pi i \sum_{m'} \delta(\varepsilon_{p'} - m'\Omega - \varepsilon_p)\Theta^{(m')}_{p'p}. \tag{7}$$

Finally, we introduce the matrix $T^{(m')}_{p'p}(E)$ depending on the energy parameter E and obeying the equation

$$T^{(m')}_{p'p}(E) = V^{(m')}_{p'p} + \sum_q \sum_n \frac{V^{(m'-n)}_{p'q}T^{(n)}_{qp}(E)}{E - (\varepsilon_q - n\Omega) + i\eta}. \tag{8}$$

Noticing that $T^{(m')}_{p'p}(E = \varepsilon_p)$ coincides with the matrix $\Theta^{(m')}_{p'p}$, we arrive at the expression

$$S_{p'p} = \delta_{p'p} - 2\pi i \sum_{m'} \delta(\varepsilon_{p'} - m'\Omega - \varepsilon_p)T^{(m')}_{p'p}(\varepsilon_p), \tag{9}$$

which relates the S matrix to the T matrix in the time-periodic case.

As follows from Eq. (9), the energy ε_p of an incoming state is conserved modulo an integer number of the drive frequency quanta, for each of which we need to find the corresponding T matrix from Eq. (8).

Let us consider a generalized version of Eq. (8)

$$T^{m'm}_{p'p}(E) = V^{m'm}_{p'p} + V^{m'n'}_{p'q'}\left[\frac{1}{E - H'_0 + i\eta}\right]^{n'n}_{q'q} T^{nm}_{qp}(E), \tag{10}$$

where $V^{m'm}_{p'p} \equiv V^{(m'-m)}_{p'p}$, and $H'_0 = H_0 - i\partial_\tau$ is the free Floquet Hamiltonian. The operator $i\partial_\tau$ is defined by $i\partial_\tau|m\rangle = m\Omega|m\rangle$ in terms of the Floquet states $|m\rangle = e^{-im\Omega\tau}$, such that $\langle m'|m\rangle = \int_0^T \frac{d\tau}{T} e^{i(m'-m)\tau} = \delta_{m'm}$. Thus, Eq. (10) is understood as a relation between operators which act in the Floquet-Hilbert space spanned by $\{|p\rangle \otimes |m\rangle\}$. For brevity we implicitly assume summations (integrations) over repeated discrete (continuous) indices.

Writing Eq. (10) in the operator form $T(E) = V + V(E - H'_0 + i\eta)^{-1}T(E)$, we can easily invert this equation and get $T(E) = V + V(E - H' + i\eta)^{-1}V$, where $H' = H'_0 + V$ is the full Floquet Hamiltonian. In the matrix representation, this solution reads

$$T^{m'm}_{p'p}(E) = V^{m'm}_{p'p} + V^{m'n'}_{p'q'}\left[\frac{1}{E - H' + i\eta}\right]^{n'n}_{q'q} V^{nm}_{qp}. \tag{11}$$

In turn, the solution of Eq. (8) $T^{(m')}_{p'p}(E) = T^{m'0}_{p'p}(E)$ is obtained from Eq. (11) in the special case $m = 0$.

Let us make the following important observation: Eq. (11) for the T matrix in the time-periodic case has almost the same form as its time-independent counterpart, the only difference consisting in additional summations over Floquet indices. Noticing that the Hamiltonian (1) conserves a number of incoming photons after scattering, we can decompose $T = \sum_{N=1}^{\infty} T_N$, where T_N is a normal ordered N-photon operator, and straightforwardly generalize the diagrammatic rules of Ref. [47]. Thus, in the time-periodic case we obtain

$$T^{m'm}_N(E) = \sum_{\{m'_j\},\{m_j\}} P_{0c} \vdots V^{m'm_1}\tilde{G}^{m_1m'_1}(E)V^{m'_1m_2}\cdots \times V^{m'_{2N-2},m_{2N-1}}\tilde{G}^{m_{2N-1},m'_{2N-1}}(E)V^{m'_{2N-1},m} \vdots P_{0c}, \tag{12}$$

given by the alternating product of $2N$ interaction operators V, and $2N-1$ dressed Green's functions $\tilde{G}(E) = (E - H'_0 - \Sigma)^{-1}$, of the cavity. Here P_0 is a projector onto the dark (i.e., nonrelaxing) state of the cavity. The Floquet components of the cavity's self-energy $\Sigma^{mm'} \equiv \Sigma^{(m-m')} = -i\pi\sum_n \langle V^{(m-n)}V^{(n-m')}\rangle_0$ are given by an average in the vacuum state of a waveguide. [In particular, for the model (1) we have $P_{0c} = |0\rangle_c\,{}_c\langle 0|$ and $\Sigma^{mm'} = -i\pi b^\dagger b\sum_n g^{(m-n)}g^{(n-m')}$]. Finally, the symbol $\vdots(\cdots)\vdots$ denotes a modified normal ordering, which ignores commutators between field operators contained in different V's, but at the same time obliges us to canonically commute a field operator contained in V with $\tilde{G}(E)$ which contains H_0.

Expression (12) is exact and sufficient to describe scattering an initial state with arbitrary number of photons. However, because of multiple summations over Floquet indices, it is not optimal for a theoretical analysis. In order to find a more convenient expression, we transform Eq. (12) into the local time representation

$$\begin{aligned} T_{N\varepsilon}(\tau) &\equiv \sum_{m'} T^{(m')}_N(E)e^{-im'\Omega\tau} \\ &= \int_0^T \frac{d\tau_1}{T}\cdots\frac{d\tau_{2N}}{T}\delta_T(\tau - \tau_1) \\ &\quad\times P_{0c}\big(\vdots V(\tau_1)\tilde{G}_\varepsilon(\tau_1,\tau_2)V(\tau_2)\cdots \\ &\quad\cdots V(\tau_{2N-1})\tilde{G}_\varepsilon(\tau_{2N-1},\tau_{2N})V(\tau_{2N})\vdots\big)P_{0c}, \end{aligned} \tag{13}$$

where we introduced the notations $\varepsilon = H_0 - E = H_0 - \varepsilon_p$ and

$$\tilde{G}_\varepsilon(\tau,\tau') = \sum_{m,m'} e^{-im\Omega\tau}\tilde{G}^{mm'}(E)e^{im'\Omega\tau'}, \tag{14}$$

and used the Poisson resummation formula

$$\sum_{m'} e^{-im'\Omega(\tau-\tau_1)} = T\sum_n \delta(\tau - \tau_1 - nT) \equiv \delta_T(\tau - \tau_1). \tag{15}$$

Then, from Eqs. (9) and (13) we deduce that the N-photon operator contribution to the nontrivial part of the scattering operator equals

$$\begin{aligned} (S-1)_N &= -i\int_{-\infty}^{\infty} d\tau e^{i(\varepsilon_{p'}-\varepsilon_p)\tau}T_{N\varepsilon}(\tau) \\ &= -i\int_{-\infty}^{\infty} d\tau e^{iH_0\tau}T_{N\varepsilon}(\tau)e^{-iH_0\tau}, \end{aligned} \tag{16}$$

and the scattering operator itself is given by

$$S = 1 + \sum_{N=1}^{\infty}(-i)\int_{-\infty}^{\infty} d\tau e^{iH_0\tau} T_{N\varepsilon}(\tau) e^{-iH_0\tau}. \quad (17)$$

Now it is necessary to establish an explicit form of $\tilde{G}_\varepsilon(\tau,\tau')$ defined in Eq. (14). From the relations

$$\sum_{m''}[(m\Omega-\varepsilon)\delta_{mm''} - \Sigma^{mm''}]\tilde{G}^{m''m'}(E) = \delta_{mm'}, \quad (18)$$

$$\sum_{m''}\tilde{G}^{mm''}(E)[(m'\Omega-\varepsilon)\delta_{m''m'} - \Sigma^{m''m'}] = \delta_{mm'}, \quad (19)$$

which are equivalent to the definition of $\tilde{G}^{mm'}(E)$, we obtain the differential equations

$$(i\partial_\tau - \varepsilon)\tilde{G}_\varepsilon(\tau,\tau') - \Sigma(\tau)\tilde{G}_\varepsilon(\tau,\tau') = \delta_T(\tau-\tau'), \quad (20)$$

$$(-i\partial_{\tau'} - \varepsilon)\tilde{G}_\varepsilon(\tau,\tau') - \tilde{G}_\varepsilon(\tau,\tau')\Sigma(\tau') = \delta_T(\tau-\tau'), \quad (21)$$

where $\Sigma(\tau) = -i\pi\langle V^2(\tau)\rangle_0 = \sum_m \Sigma^{(m)} e^{-im\Omega\tau}$. Equipping them with the periodic boundary conditions in both variables, we find a solution

$$\tilde{G}_\varepsilon(\tau,\tau') = -iT\sum_n \Theta(\tau-\tau'-nT)e^{-i\bar{\varepsilon}(\tau-\tau'-nT)} \times e^{-F_{\rm osc}(\tau)+F_{\rm osc}(\tau')}, \quad (22)$$

where $\bar{\varepsilon} = \varepsilon + \Sigma^{(0)}$ and $F_{\rm osc}(\tau) = -\sum_{m\neq 0}\frac{\Sigma^{(m)}}{m\Omega}e^{-im\Omega\tau}$. Inserting it into Eq. (13) and extending the finite integration ranges $0 < \tau_j < T$ to the infinite ones $-\infty < t_j < \infty$, we cast the scattering operator (17) to the form

$$S = 1 + \sum_{N=1}^{\infty}(-i)^{2N}\int dt_1\cdots dt_{2N}\Theta(t_1 > \cdots > t_{2N}) \times e^{i(H_0-E)t_1}P_{0c}\big([t]\vdots V(t_1)e^{-F(t_1)}e^{F(t_2)}V(t_2)e^{-F(t_2)}\cdots \times V(t_{2N-1})e^{-F(t_{2N-1})}e^{F(t_{2N})}V(t_{2N})\,[t]\vdots\big)P_{0c}, \quad (23)$$

where $F(t) = i(H_0 + \Sigma^{(0)} - E)t + F_{\rm osc}(t)$, and E is the energy of an input state. In the following we identify S with ${}_c\langle 0|S|0\rangle_c$.

Note that an N-photon operator from the above sum gives only nonzero contribution, if it is applied to an M-photon initial state such that $N \leqslant M$. This means that for an M-photon initial state the sum can be truncated after the Mth term. To illustrate an application of Eq. (23) we consider in the next section examples of a single- and two-photon scattering in the model (1).

III. FEW-PHOTON SCATTERING

Let us consider the model (1) and assume that an initial state is prepared in a form of a coherent rectangular pulse of length L, which is initially located far left from the cavity and starts moving toward it in the right direction with a constant velocity v. In the interaction picture, this initial state is expressed by

$$|\Psi_i\rangle = e^{-|\alpha|^2/2}e^{\alpha\mathcal{A}^\dagger_{r,\omega_0}}|0\rangle, \quad (24)$$

where $\mathcal{A}_{r,\omega_0} = \int d\omega\phi(\omega)a_{r\omega}$ is a normalized wave-packet operator centered around the mode ω_0 and broadened over the width $\sim \frac{2\pi v}{L}$. Formally it is defined by the function

$$\phi(\omega) = \sqrt{\frac{2v}{\pi L}}\frac{\sin\frac{L}{2v}(\omega-\omega_0)}{\omega-\omega_0}, \quad (25)$$

which approaches $\sqrt{\frac{2\pi v}{L}}\delta(\omega-\omega_0)$ for long pulses.

For weak coherence $|\alpha| \ll 1$ we approximate the state (24) by

$$|\Psi_i\rangle \approx e^{-|\alpha|^2/2}\left[1 + \alpha\mathcal{A}^\dagger_{r,\omega_0} + \alpha^2\frac{(\mathcal{A}^\dagger_{r,\omega_0})^2}{2}\right]|0\rangle. \quad (26)$$

Both single- and two-photon states contributing to Eq. (26) have a well-defined energy in the long pulse limit $L\to\infty$, and therefore we can apply the scattering operator (23) to each of them, thus obtaining a final state $|\Psi_f\rangle = S|\Psi_i\rangle$ in the two-photon approximation.

We are interested in computing—to the leading order in α—the average transmitted and reflected fields and their statistical properties quantified by the second-order coherence function $g^{(2)}$. In particular, defining the field operators in the coordinate representation

$$a_\sigma(x) = \frac{1}{\sqrt{2\pi v}}\int d\omega a_{\sigma\omega}e^{i\omega x/v}, \quad \sigma = r,l, \quad (27)$$

we wish to find $\langle\Psi_f|a_\sigma(x-vt)|\Psi_f\rangle$ and

$$g^{(2)}_{\sigma\sigma'}(t,\tau_d) = \frac{G^{(2)}_{\sigma\sigma'}(t,\tau_d)}{g^{(1)}_\sigma(t)g^{(1)}_{\sigma'}(t+\tau_d)}, \quad (28)$$

where

$$G^{(2)}_{\sigma\sigma'}(t,\tau_d) = \langle\Psi_f|a^\dagger_\sigma(x-vt)a^\dagger_{\sigma'}(x-vt-v\tau_d) \times a_{\sigma'}(x-vt-v\tau_d)a_\sigma(x-vt)|\Psi_f\rangle, \quad (29)$$

$$g^{(1)}_\sigma(t) = \langle\Psi_f|a^\dagger_\sigma(x-vt)a_\sigma(x-vt)|\Psi_f\rangle, \quad (30)$$

and τ_d is a delay time.

Because of an explicit time dependence in the Hamiltonian (1), there is no time translational invariance in the long time limit (a corresponding system's state is therefore said to be *quasistationary*), and the above-defined functions also depend on the evolution time t (though in a periodic way, as we will see later). Note that the definition (27) implies that the x axis for left-moving photons ($\sigma = l$) points in the left direction.

Since in the Hamiltonian (1) only even states ($a_\omega = \frac{a_{r\omega}+a_{l\omega}}{\sqrt{2}}$) are coupled to the cavity, and odd states ($\tilde{a}_\omega = \frac{a_{r\omega}-a_{l\omega}}{\sqrt{2}}$) are decoupled from it, it appears convenient to express the scattering operator in the basis of even states, also representing the initial state (26) in terms of even and odd states. A task of finding $|\Psi_f\rangle$ essentially reduces to evaluation of $S\mathcal{A}^\dagger_{\omega_0}|0\rangle$ and $S\frac{1}{2}(\mathcal{A}^\dagger_{\omega_0})^2|0\rangle$, where $\mathcal{A}_{\omega_0}$ is an even counterpart of $\mathcal{A}_{r,\omega_0}$. We consider these cases of single- and two-photon scattering in the following sections.

A. Single-photon scattering

Let us first establish how the scattering operator (23) acts on a single-photon plane-wave even state $a^\dagger_\omega|0\rangle$ with energy

$E = \omega$. Truncating the sum in Eq. (23) at $N = 1$, we obtain

$$
\begin{aligned}
&Sa^\dagger_\omega|0\rangle \\
&= a^\dagger_\omega|0\rangle - \int dt_1 dt_2 \Theta(t_1 > t_2) \int d\omega_1 \int d\omega_2 e^{i(\omega_1-\omega)t_1} \\
&\quad \times {}_c\langle 0|\big([t]\vdots g(t_1) a^\dagger_{\omega_1} b e^{-F(t_1)} e^{F(t_2)} g(t_2) b^\dagger a_{\omega_2} [t]\vdots\big)|0\rangle_c \, a^\dagger_\omega|0\rangle \\
&= a^\dagger_\omega|0\rangle - \int d\omega_1 \int_{-\infty}^{\infty} dt_1 e^{i(\omega_1-\omega)t_1} g(t_1) e^{-f_{1\omega}(t_1)} \\
&\quad \times \int_{-\infty}^{t_1} dt_2 e^{f_{1\omega}(t_2)} g(t_2) a^\dagger_{\omega_1}|0\rangle \\
&\equiv \int d\omega_1 [\delta_{\omega_1\omega} + s_{\omega_1\omega}] a^\dagger_{\omega_1}|0\rangle. \qquad (31)
\end{aligned}
$$

The function $F(t)$ for the model (1) acquires the form

$$F(t) = i(H_0 - i\Gamma^{(0)} b^\dagger b - E)t + f_{\rm osc}(t) b^\dagger b, \qquad (32)$$

where $\Gamma^{(0)} + \dot f_{\rm osc}(t) = \pi g^2(t) \equiv \Gamma(t)$, and $f_{\rm osc}(t)$ is fixed by the condition that it does not have a zero frequency component. To single-photon scattering contributes only a single-excitation component $\langle 1|F(t)|1\rangle$, and its contribution is appropriately written in terms of the functions $f_{1\omega}(t) = i(\omega_c - i\Gamma^{(0)} - \omega)t + f_{\rm osc}(t)$.

Folding Eq. (31) with the wave packet $\phi(\omega)$ and applying the field operator $a(x - vt)$ to the obtained single-photon scattering state, we find

$$a(x - vt) S\mathcal{A}^\dagger_{\omega_0}|0\rangle = \frac{e^{-i\omega_0 t_x}}{\sqrt{L}}[1 + 2A(t_x)]|0\rangle, \qquad (33)$$

$$A(t_x) = -\pi g(t_x) e^{-f_1(t_x)} \int_{-\infty}^{t_x} dt' e^{f_1(t')} g(t'), \qquad (34)$$

where t is time elapsed since the beginning of the interaction and $t_x = t - x/v$ is a time lag between the pulse front and the field at point x. In Eq. (34) we have also introduced

$$f_1(t) \equiv f_{1\omega_0}(t) = -i(\delta + i\Gamma^{(0)})t + f_{\rm osc}(t), \qquad (35)$$

with the detuning $\delta = \omega_0 - \omega_c$. The function $A(t_x)$ is periodic in its argument, $A(t_x) = A(t_x + T)$, and therefore we can reduce the central time of pulse evolution t_x (in other words, the observation time at point x) to a single period: $t_x \to \tau_c \in [-T/2, T/2]$.

Transforming Eq. (33) to the basis of right and left modes, we obtain the transmitted field (labeled by r, the direction of the incident field) and the reflected field (labeled by l, the opposite direction)

$$
\begin{aligned}
a_{r,l}(-vt_x) S\mathcal{A}^\dagger_{r,\omega_0}|0\rangle &= \frac{a(-vt_x) \pm \tilde a(-vt_x)}{\sqrt{2}} \frac{S\mathcal{A}^\dagger_{\omega_0} + \tilde{\mathcal{A}}^\dagger_{\omega_0}}{\sqrt{2}}|0\rangle \\
&= \frac{e^{-i\omega_0 t_x}}{\sqrt{L}}\left[\frac{1 \pm 1}{2} + A(t_x)\right]|0\rangle. \qquad (36)
\end{aligned}
$$

The transmission $t(\tau_c) = 1 + A(\tau_c)$ and reflection $r(\tau_c) = A(\tau_c)$ amplitudes give envelope shapes of the corresponding fields, and they are not constant in time. Nevertheless, they obey the normalization condition

$$\frac{1}{T}\int_0^T d\tau_c (|t(\tau_c)|^2 + |r(\tau_c)|^2) = 1, \qquad (37)$$

corresponding to a conservation of the photon number (see Appendix A for the proof). In the linear regime, one can relate the transmission and reflection amplitudes to the equal-time first-order coherences of Eq. (30) by

$$g^{(1)}_r(\tau_c) = \frac{|\alpha|^2}{L}|t(\tau_c)|^2, \quad g^{(1)}_l(\tau_c) = \frac{|\alpha|^2}{L}|r(\tau_c)|^2. \qquad (38)$$

Periodic time dependence of an envelope of a scattered field is the main effect of a periodic time modulation of coupling seen in a single-photon scattering. In the following we study this dependence for different modulation protocols. To evaluate $A(\tau_c)$ for $\tau_c \in [-T/2, T/2]$ in practice, it is convenient to split the integral range $[-\infty, \tau_c]$ in Eq. (34) into two ranges $[-\infty, -T/2]$ and $[-T/2, \tau_c]$. The integral over the second range can be evaluated numerically, while the integral over the first range can be converted into a geometric series by using the periodicity of $g(t)$ and $f_{\rm osc}(t)$ which results in

$$\int_{-\infty}^{-T/2} dt' e^{-i(\delta + i\Gamma^{(0)})t'} e^{f_{\rm osc}(t')} g(t') = \frac{C_0}{e^{-i(\delta + i\Gamma^{(0)})T} - 1}. \qquad (39)$$

Here $C_0 = \int_{-T/2}^{T/2} dt' e^{-i(\delta + i\Gamma^{(0)})t'} e^{f_{\rm osc}(t')} g(t')$ is also evaluated numerically.

Before choosing specific protocols $g(t)$, let us first analyze under which conditions one can expect an interesting time behavior of an envelope A. The most trivial time dependence appears in the case of slow driving, when $A(\tau_c)$ instantaneously follows $g(\tau_c)$. It is captured by applying the adiabatic approximation to Eq. (34), which is achieved by expanding the integrand close to the upper limit given by the time of observation τ_c. Physically this means that a protocol's history influences very little the present time value of A. We have

$$
\begin{aligned}
A(\tau_c) &= -\pi g(\tau_c) \int_{-\infty}^{0} d\tau e^{f_1(\tau_c+\tau) - f_1(\tau_c)} g(\tau_c + \tau) \\
&\approx -\pi g(\tau_c) \int_{-\infty}^{0} d\tau e^{\dot f_1(\tau_c)\tau} \\
&\quad \times \left[g(\tau_c) + \dot g(\tau_c)\tau + \frac{1}{2} g(t_x) \ddot f_1(\tau_c)\tau^2\right]. \qquad (40)
\end{aligned}
$$

Noticing that $\dot f_1(\tau_c) = -i[\delta + i\Gamma(\tau_c)]$, we conclude

$$A(\tau_c) \approx -\frac{i\Gamma(\tau_c)}{\delta + i\Gamma(\tau_c)}\left[1 - \frac{i\dot g(\tau_c)}{g(\tau_c)} \frac{\delta - i\Gamma(\tau_c)}{[\delta + i\Gamma(\tau_c)]^2}\right]. \qquad (41)$$

The leading term gives the instantaneous amplitude, and the second term represents the adiabatic correction. This approximation is valid as long as the adiabaticity condition

$$\left|\frac{\dot g(t)}{g(t)}\right| \ll \sqrt{\delta^2 + \Gamma^2(t)} \qquad (42)$$

is fulfilled. Interesting and unexpected behavior shows up when this condition is violated as we explore in further detail in Sec. IV.

B. Two-photon scattering

Applying the scattering operator (23) to the two-photon state with energy $E = \omega + \omega'$ we obtain

$$Sa^\dagger_\omega a^\dagger_{\omega'}|0\rangle = \frac{1}{2}a^\dagger_\omega a^\dagger_{\omega'}|0\rangle + \int d\omega_1 s_{\omega_1\omega} a^\dagger_{\omega_1} a^\dagger_{\omega'}|0\rangle + \int d\omega_1 d\omega_2 d\omega_3 d\omega_4 \int dt_1 dt_2 dt_3 dt_4 \Theta(t_1 > t_2 > t_3 > t_4) e^{i(H_0-E)t_1}$$
$$\times {}_c\langle 0|\big([t]\vdots g(t_1)a^\dagger_{\omega_1} b e^{-F(t_1)} e^{F(t_2)} g(t_2) b^\dagger a_{\omega_3} e^{-i(H_0-E)(t_2-t_3)} g(t_3) a^\dagger_{\omega_2} b e^{-F(t_3)} e^{F(t_4)} g(t_4) b^\dagger a_{\omega_4} [t]\vdots$$
$$+ [t]\vdots g(t_1)a^\dagger_{\omega_1} b e^{-F(t_1)} e^{F(t_2)} g(t_2) a^\dagger_{\omega_2} b e^{-F(t_2)} e^{F(t_3)} g(t_3) b^\dagger a_{\omega_3} e^{-F(t_3)} e^{F(t_4)} g(t_4) b^\dagger a_{\omega_4} [t]\vdots\big)|0\rangle_c a^\dagger_\omega a^\dagger_{\omega'}|0\rangle + (\omega \leftrightarrow \omega'). \tag{43}$$

The $N = 2$ contribution is represented by the two terms populating the cavity with at most one photon ($\sim bb^\dagger bb^\dagger$) and with two photons ($\sim bbb^\dagger b^\dagger$). Simplifying Eq. (43) (see Appendix B) we obtain

$$a(-vt_x - v\tau_d)a(-vt_x)S\frac{\mathcal{A}^{\dagger 2}_{\omega_0}}{2}|0\rangle = \frac{e^{-i\omega_0(2t_x+\tau_d)}}{L}[1 + 2A(t_x) + 2A(t_x+\tau_d) + 4\bar{B}(t_x,\tau_d)]|0\rangle, \tag{44}$$

where

$$\bar{B}(t_x,\tau_d) = B(t_x,\tau_d) + A(t_x)A(t_x+\tau_d), \tag{45}$$

$$B(t_x,\tau_d) = -iUg(t_x)e^{-f_1(t_x)}g(t_x+\tau_d)e^{-f_1(t_x+\tau_d)}\int_{-\infty}^{t_x} dt' e^{iU(t'-t_x)+2f_1(t')}\frac{A^2(t')}{g^2(t')}. \tag{46}$$

The function B in Eq. (46) is associated with an inelastic contribution to the two-photon scattering: it vanishes for $U = 0$. It is periodic in the argument t_x, therefore we can again make a replacement $t_x \to \tau_c$. For the time-independent coupling we recover the expression

$$B(\tau_d) = -A^2\frac{U}{U - 2(\delta + i\Gamma)}e^{i(\delta+i\Gamma)\tau_d}. \tag{47}$$

In the large U limit, which corresponds to the case of a two-level system, the inelastic contribution (46) becomes equal (see Appendix B)

$$B(t_x,\tau_d) = -\frac{g(t_x+\tau_d)}{g(t_x)}A^2(t_x)e^{f_{\rm osc}(t_x)-f_{\rm osc}(t_x+\tau_d)}e^{i(\delta+i\Gamma)\tau_d}. \tag{48}$$

With help of Eq. (44) we find analogous expressions for transmitted and reflected fields

$$a_r(-vt_x - v\tau_d)a_r(-vt_x)S\frac{\mathcal{A}^{\dagger 2}_{r,\omega_0}}{2}|0\rangle$$
$$= \frac{e^{-i\omega_0(2t_x+\tau)}}{L}[t(t_x)t(t_x+\tau_d) + B(t_x,\tau_d)]|0\rangle, \tag{49}$$
$$a_l(-vt_x - v\tau_d)a_l(-vt_x)S\frac{\mathcal{A}^{\dagger 2}_{r,\omega_0}}{2}|0\rangle$$
$$= \frac{e^{-i\omega_0(2t_x+\tau_d)}}{L}[r(t_x)r(t_x+\tau_d) + B(t_x,\tau_d)]|0\rangle, \tag{50}$$

which allow us to define the corresponding second-order coherence functions

$$g^{(2)}_{rr}(\tau_c,\tau_d) = \left|1 + \frac{B(\tau_c,\tau_d)}{t(\tau_c)t(\tau_c+\tau_d)}\right|^2, \tag{51}$$
$$g^{(2)}_{ll}(\tau_c,\tau_d) = \left|1 + \frac{B(\tau_c,\tau_d)}{r(\tau_c)r(\tau_c+\tau_d)}\right|^2. \tag{52}$$

IV. RESULTS

A. Reflection and transmission

Assuming a weakly coherent initial signal in the right-moving mode a_{r,ω_0}, we study in this section the linear reflection $r(\tau_c) = A(\tau_c)$ and transmission $t(\tau_c) = 1 + A(\tau_c)$, which are periodic functions of the reduced central time $\tau_c \in [-T/2, T/2]$. Their absolute values give envelope shapes of average reflected and transmitted fields, periodically changing in space and time. This behavior contrasts with the case time-independent coupling featuring constant $r = -\frac{i\Gamma}{\delta+i\Gamma}$ and $t = \frac{\delta}{\delta+i\Gamma}$.

We apply the general results of Sec. III to two coupling modulation protocols: (1) "on-off" $g(t) = g_0(1 + \cos\Omega t)$; and (2) "sign change" $g(t) = g_0\cos\Omega t$. In the on-off protocol the coupling strength is periodically quenched to zero [Fig. 2(a)], while in the sign-change protocol, the sign of $g(t)$ changes after crossing zero [Fig. 2(c)]. A notable difference between the two protocols is that the former yields a 2π-periodic modulation of a field's amplitude [Fig. 2(b)], while the latter yields a π-periodic one [Fig. 2(d)].

For a time-independent interaction, a single photon on resonance ($\delta = 0$) is fully reflected ($r = -1$), regardless the value of the coupling strength. Should the adiabaticity condition (42) be fulfilled at every time t for a time periodic interaction, we would expect the reflection amplitude $r(t)$ to follow $\Gamma(t)$ instantaneously [see Eq. (41)], also showing (almost) full reflection in the resonant case (up to a small fraction $\sim |\dot{g}(t)/[g(t)\Gamma(t)]|$ of the transmitted photon's probability density). However, the adiabaticity condition (42) is strongly violated for these two protocols. For any protocol with a momentary quench of coupling this can happen even at slow driving. In these cases the nonadiabatic behavior of A does depend on a protocol's history as we shall see later.

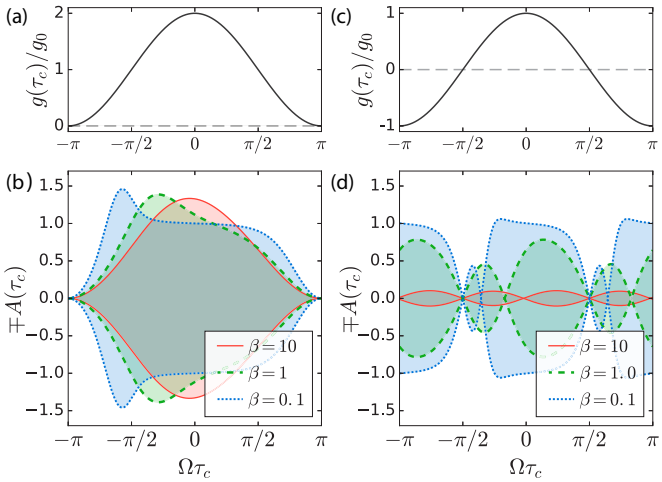

FIG. 2. Envelopes of the reflected field. (a) The on-off cosine signal, and the resulting (b) envelope as a function of the central time τ_c for various driving speeds. Note the perfect transmission ($A = 0$) when the coupling is quenched. (c) The sign-change cosine signal and the resulting (d) envelope. The envelope repeats itself after a half period, and in addition to the two coupling quench nodes at $\Omega\tau_c = \pm\pi/2$ an extra node develops at $\Omega\tau_c \approx -\pi/2$ (at slow drive) and moves toward $\tau_c = 0$ (at fast drive).

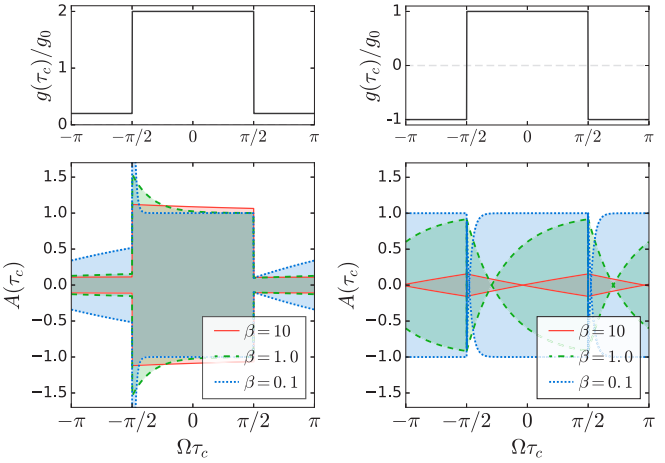

FIG. 3. Envelope function $A(\tau_c)$ for rectangular driving procedures, which are nonsmooth versions of the on-off and sign-change protocols in Fig. 2. The off component of the on-off signal has been set at (a more realistic) small nonzero value, $g_{\rm off} = g_0/5$.

Moreover, at certain time instants the coupling strength in both of them is quenched, implying a momentary decoupling of microwave photons from the cavity and hence full transmission at these time instants. Since we are dealing with an open quantum system, this qualitative picture becomes even more complicated due to memory effects, and the nonadiabatic behavior can be explained as a sum over histories. Each history has the photon entering the cavity at some initial time τ_i and leaving at some later time τ_f, with an amplitude $g(\tau_i)g(\tau_f)$ and a weight determined by the decay probability of the photonic state in the cavity, $\exp(-\int_{\tau_i}^{\tau_f}\Gamma(\tau)d\tau)$. The reflection coefficient at τ_f, given by the sum over initial times τ_i, is highly influenced by the evolution within a memory window set by the decay rate of the cavity.

In the on-off protocol the memory window is largest for final times after the $\Omega\tau_c = -\pi$ node, meaning that the photon remains longer in the cavity and is released shortly after when the coupling strength is sufficiently increased, producing a spike in the reflection coefficient that overshoots unity [Fig. 2(b)]. In the sign-change protocol, memory effects create an additional node, which is absent in $g(t)$, close to $\Omega\tau_c = -\pi/2$ for slow drive, and moving toward $\tau_c = 0$ for faster drives [Fig. 2(d)]. For times shortly after the $-\pi/2$ node of $g(t)$ the memory window includes histories with amplitudes of opposite signs, and their competition creates this additional node. These two examples show how different protocols may not only chop the wave packet of the incoming photon, but also significantly alter its form.

The resulting envelopes strongly depend on the normalized frequency $\beta = \Omega/\Gamma^{(0)}$, where $\Gamma^{(0)}$ is the zeroth harmonic of $\Gamma(t)$. For the fast drive $\beta \gg 1$, we obtain $A(\tau_c) \approx -\frac{2}{3}(1 + \cos\Omega\tau_c)$ in the on-off protocol, which means that the reflected pulse follows $g(\tau_c)$, not $\Gamma(\tau_c)$; and $A(\tau_c) \approx -\frac{1}{\beta}\sin 2\Omega\tau_c$ following $\Gamma^{(0)}\tau_c - f_1(\tau_c)$ in the sign-change protocol. In the second case, $A(\tau_c)$ is negligibly small, so that we have (almost) full transmission despite the resonance—this effect is in sharp contrast to its nondriven counterpart, where the full reflection is expected. Thus, this protocol can be used for the dynamical routing of photons. For slow drive, $\beta \ll 1$, the adiabaticity condition is fulfilled at least within some range around $\tau_c = 0$, and this accounts for the formation of a plateau with $A(\tau_c) \approx -1$, resembling full reflection in the nondriven resonant case.

As we have seen above, a momentary quench of coupling leads to a formation of nodes in the reflected field. This effect can be viewed as the quantum version of optical chopping. It is a quantum effect because a scattered single photon remains in a linear superposition of its transmitted and reflected states. It is analogous to chopping because the amplitude of the transmitted signal is periodically changed from its maximal value down to zero and back again.

To make this analogy more obvious we show in Fig. 3 the single-photon reflection amplitudes in the resonant case $\delta = 0$ for rectangular driving procedures that more closely resemble the operation of a conventional chopper: on the figure at $|g| \sim g_0$ the photon passage is shut (full reflection), while at $|g| \ll g_0$ it is open (full transmission). The envelope function $A(\tau_c)$ shows qualitatively the same effects as for the cosine signal investigated above. Note that at large β (fast drive), the signal shaping also works for the on-off procedure, as it does for the cosine signal.

B. Second-order coherence

The second-order coherences in Eq. (28) manifest nonlinear effects quantified by the value of U. Only fast drives, $\beta = \Omega/\Gamma^{(0)} \gg 1$, are able to affect the correlations before they decay, and we numerically calculate $g_{ll}^{(2)}$ for fast and moderate drives in the two cosine protocols. In the on-off protocol, the fast drive only induces small oscillations in the correlation function around the nondriven results, as shown in Fig. 4.

In contrast, the sign-change protocol induces huge bunching effects due to the additional node in the single-photon

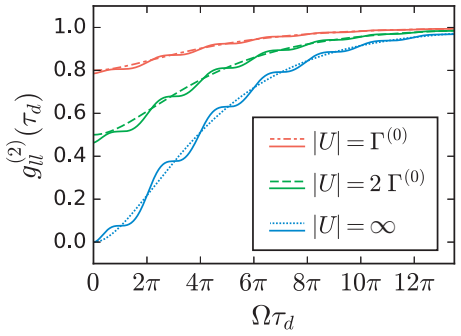

FIG. 4. The $g_{ll}^{(2)}(\tau_c = 0, \tau_d)$ correlation function for the on-off protocol at fast driving, $\beta = 10$. The $g^{(2)}$ correlations for the corresponding nondriven system with a decay rate set to $\Gamma^{(0)}$ are shown as dashed lines, and the (uninteresting) correlations for the driven system slightly oscillate around the nondriven antibunching curves.

reflection, as can be clearly seen in Fig. 5(a). We also find periodic oscillations between strong bunching (red areas) and antibunching (blue areas) away from $\Omega\tau_c = 0$ and $\Omega\tau_c = \pm\pi$. This is a dramatic change in statistical properties of the reflected light due to the time dependence of $g(t)$ as compared to the case of constant g, where $g_{ll}^{(2)}$ is monotonously antibunched. For a moderate drive, $\beta = 1$, all oscillatory effects in the sign-change protocol die out for delay times longer than a single drive period, as shown in Fig. 5(b).

The photon compression by the on-off driving introduces nodes in the transmission and produces, similar to the field quench effects in the reflected light for the sign-change protocol, strong bunching in the transmitted light captured by $g_{rr}^{(2)}$. This picture is verified by a numerical calculation of the correlation function for fast drive, $\beta = 10$, and nonlinearity, $|U| = 2\Gamma^{(0)}$, as shown in Fig. 6.

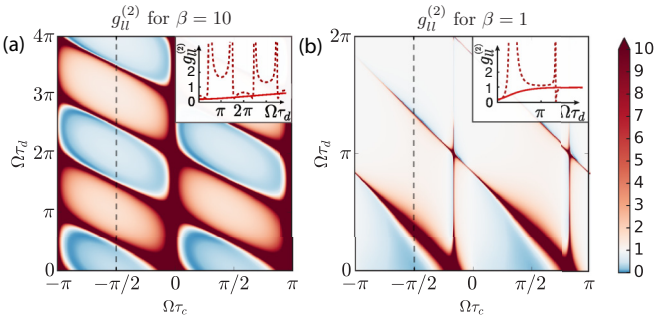

FIG. 5. Second-order coherence of the reflected pulse $g_{ll}^{(2)}$ in the sign-change protocol as a function of central time τ_c and delay time τ_d for the Kerr nonlinearity $|U| = 4\Gamma^{(0)}$. We show results for (a) the fast drive $\beta = 10$, where huge periodically repeated bunching peaks are formed and interwoven with areas of moderate bunching and antibunching; (b) the intermediate drive $\beta = 1$, showing the decay of $g_{ll}^{(2)}$ to the uncorrelated value (white area). Insets: Comparison of the cuts at $\Omega\tau_c = -\frac{\pi}{2}$ (dashed line) with the unmodulated $g_{ll}^{(2)}$ (solid line).

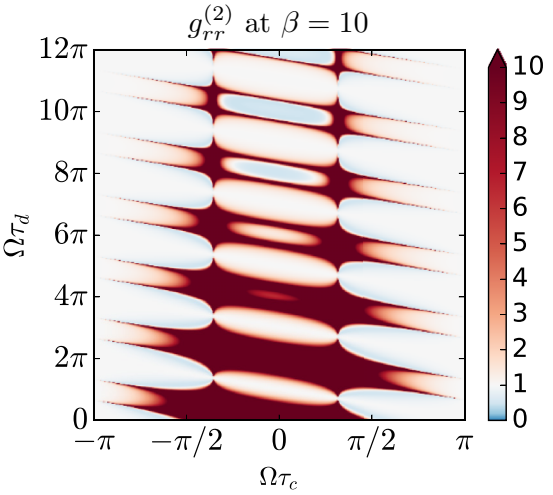

FIG. 6. The $g_{rr}^{(2)}$ correlation of transmitted light in the on-off protocol at fast driving, $\beta = 10$, with a nonlinearity $|U| = 2\Gamma^{(0)}$. Note the strong periodically recurring bunching due to the wave-packet compression.

V. SUMMARY

We have proposed a quantum analog of an optical chopper, operating at the few-photon level and realizable by a time-periodic modulation of the photon emitter coupling. We have developed an exact Floquet scattering approach based on diagrammatic scattering theory and applied it to quantitatively describe scattering of microwave photons from the nonlinear cavity in two driving protocols of the coupling: on-off and sign change. In both of them we have observed interesting nonadiabatic memory effects arising due to the driving. In particular, the on-off protocol produces periodic compressions of the photon's wave packet at slow drive, while at fast drive the signal is directly encoded into the shape of the single-photon pulse. The sign-change protocol in turn gives rise to the additional nodes in the envelope at which the field is completely quenched, while at fast drive it may completely change the direction of a photon. These are two examples of chopping realizable at the quantum single-photon level. In addition, in the latter protocol we find dramatic changes in statistical properties of the reflected field showing up as strong bunching peaks in the $g^{(2)}$ function that are interwoven with periodically alternating areas of antibunching and moderate bunching—features that are in sharp contrast to their nondriven counterparts. Thus, our findings can be useful for single-photon pulse shaping, dynamical routing of photons, and altering of the photon statistics in real time.

ACKNOWLEDGMENTS

We are grateful to A. Fedorov and M. Hafezi for useful discussions. The work of V.G. is a part of the Delta-ITP consortium, a program of the Netherlands Organization for Scientific Research (NWO) that is funded by the Dutch Ministry of Education, Culture and Science (OCW).

APPENDIX A: PROOF OF THE NORMALIZATION CONDITION

To prove the normalization condition (37) we need to show that

$$\int_0^T d\tau_c |A(\tau_c)|^2 = -\mathrm{Re}\int_0^T d\tau_c A(\tau_c). \tag{A1}$$

Let us introduce the function

$$W(t) = \int_{-\infty}^{t} dt' e^{f_1(t')} g(t') \equiv -\frac{A(t)}{\pi g(t)} e^{f_1(t)}. \tag{A2}$$

Noticing that $\frac{d}{dt}[f_1(t) + f_1^*(t)] = 2\Gamma(t) = 2\pi g^2(t)$ we integrate the left-hand side of Eq. (A1) by parts:

$$\int_0^T d\tau_c \pi \Gamma(\tau_c) e^{-[f_1(\tau_c)+f_1^*(\tau_c)]} |W(\tau_c)|^2 = -\frac{\pi}{2} e^{-[f_1(\tau_c)+f_1^*(\tau_c)]} |W(\tau_c)|^2 \Big|_0^T + \frac{\pi}{2}\int_0^T d\tau_c e^{-[f_1(\tau_c)+f_1^*(\tau_c)]} \times [\dot{W}^*(\tau_c) W(\tau_c) + W^*(\tau_c)\dot{W}(\tau_c)]. \tag{A3}$$

The first term vanishes because of the periodicity of the function $e^{-f_1(t)}W(t)$, while the second term amounts to

$$\frac{\pi}{2}\int_0^T d\tau_c g(\tau_c)[e^{-f_1(\tau_c)} W(\tau_c) + e^{-f_1^*(\tau_c)} W^*(\tau_c)], \tag{A4}$$

which coincides with the right-hand side of Eq. (A1). Thus, Eq. (37) is fulfilled.

APPENDIX B: EVALUATION OF THE TWO-PHOTON SCATTERING STATE

The form of the two-photon scattering state in Eq. (43) can be reduced to

$$\begin{aligned} S a_\omega^\dagger a_{\omega'}^\dagger |0\rangle = {} & \frac{1}{2} a_\omega^\dagger a_{\omega'}^\dagger |0\rangle + \int d\omega_1 s_{\omega_1\omega} a_{\omega_1}^\dagger a_{\omega'}^\dagger |0\rangle + \int d\omega_1 d\omega_2 \int dt_1 dt_2 dt_3 dt_4 \Theta(t_1 > t_2 > t_3 > t_4) e^{i(\omega_1+\omega_2-\omega-\omega')t_1} \\ & \times [g(t_1) e^{-f_{1,E-\omega_2}(t_1)} e^{f_{1,E-\omega_2}(t_2)} g(t_2) e^{-i(\omega_2-\omega')(t_2-t_3)} g(t_3) e^{-f_{1\omega'}(t_3)} e^{f_{1\omega'}(t_4)} g(t_4) \\ & + 2 g(t_1) e^{-f_{1,E-\omega_2}(t_1)} e^{f_{1,E-\omega_2}(t_2)} g(t_2) e^{-f_2(t_2)} e^{f_2(t_3)} g(t_3) e^{-f_{1\omega'}(t_3)} e^{f_{1\omega'}(t_4)} g(t_4)] a_{\omega_1}^\dagger a_{\omega_2}^\dagger |0\rangle + (\omega \leftrightarrow \omega'), \end{aligned} \tag{B1}$$

where $f_2(t) = i(2\omega_c + U - 2i\Gamma^{(0)} - \omega - \omega')t + 2f_{\mathrm{osc}}(t)$. Folding it with $\phi(\omega)\phi(\omega')$ and applying the field operators $a(-vt_x - v\tau_d)a(-vt_x)$ we obtain expression (44) with

$$\begin{aligned} 4\bar{B}(t_x,\tau_d) = {} & \int d\omega_1 d\omega_2 \int dt_1 dt_2 dt_3 dt_4 \Theta(t_1 > t_2 > t_3 > t_4) e^{i(\omega_1-\omega_0)t_1} e^{i(\omega_2-\omega_0)t_2} \\ & \times [g(t_1) e^{-f_1(t_1)} e^{f_1(t_2)} g(t_2) e^{-i(\omega_2-\omega_0)(t_2-t_3)} g(t_3) e^{-f_1(t_3)} e^{f_1(t_4)} g(t_4) \\ & + 2 e^{-iU(t_2-t_3)} g(t_1) e^{-f_1(t_1)} e^{f_1(t_2)} g(t_2) e^{-2f_1(t_2)} e^{2f_1(t_3)} g(t_3) e^{-f_1(t_3)} e^{f_1(t_4)} g(t_4)] \\ & \times (e^{-it_x(\omega_1-\omega_0)} e^{-i(t_x+\tau_d)(\omega_2-\omega_0)} + e^{-it_x(\omega_2-\omega_0)} e^{-i(t_x+\tau_d)(\omega_1-\omega_0)}), \end{aligned} \tag{B2}$$

and $f_1(t)$ defined in Eq. (35). Performing frequency integrals in Eq. (B2) simplifies it to

$$\begin{aligned} \bar{B}(t_x,\tau_d) = {} & \pi^2 g(t_x+\tau_d) e^{-f_1(t_x+\tau_d)} g(t_x) e^{-f_1(t_x)} \int dt_2 dt_4 e^{f_1(t_4)} g(t_4) e^{f_1(t_2)} g(t_2) \\ & \times [\Theta(t_x+\tau_d > t_2 > t_x)\Theta(t_x > t_4) + 2\Theta(t_x > t_2 > t_4) e^{-iU(t_x-t_2)}]. \end{aligned} \tag{B3}$$

The second integral containing the U-dependent phase factor can be written in terms of function (A2) as

$$\int_{-\infty}^{t_x} dt_2 2\dot{W}(t_2) W(t_2) e^{-iU(t_x-t_2)} = W^2(t_x) - iU\int_{-\infty}^{t_x} dt_2 W^2(t_2) e^{-iU(t_x-t_2)}. \tag{B4}$$

Representing

$$W^2(t_x) = \int_{-\infty}^{t_x} dt_2 e^{f_1(t_2)} g(t_2) \int_{-\infty}^{t_x} dt_4 e^{f_1(t_4)} g(t_4), \tag{B5}$$

we substitute Eq. (B4) in Eq. (B3) and obtain

$$\bar{B}(t_x,\tau) = \pi^2 g(t_x+\tau_d) e^{-f_1(t_x+\tau_d)} g(t_x) e^{-f_1(t_x)} \left[\int_{-\infty}^{t_x+\tau_d} dt_2 e^{f_1(t_2)} g(t_2) \int_{-\infty}^{t_x} dt_4 e^{f_1(t_4)} g(t_4) - iU\int_{-\infty}^{t_x} dt_2 W^2(t_2) e^{-iU(t_x-t_2)}\right], \tag{B6}$$

which is equivalent to Eqs. (45) and (46). Note that the contribution (B4) to the inelastic part of $g^{(2)}$ vanishes in the limit $|U| \to \infty$ (rapid oscillations average the integral in the left-hand side to zero). Thus, we obtain Eq. (48).

[1] P. L. Kapitza, Dynamic stability of a pendulum when its point of suspension vibrates, Sov. Phys. JETP **21**, 588 (1951).

[2] N. H. Lindner, G. Refael, and V. Galitski, Floquet topological insulator in semiconductor quantum wells, Nat. Phys. **7**, 490 (2011).

[3] T. Kitagawa, T. I. Oka, A. Brataas, L. Fu, and E. Demler, Transport properties of nonequilibrium systems under the application of light: Photoinduced quantum Hall insulators without Landau levels, Phys. Rev. B **84**, 235108 (2011).

[4] T. Kitagawa, E. Berg, M. Rudner, and E. Demler, Topological characterization of periodically driven quantum systems, Phys. Rev. B **82**, 235114 (2010).

[5] N. Goldman and J. Dalibard, Periodically Driven Quantum Systems: Effective Hamiltonians and Engineered Gauge Fields, Phys. Rev. X **4**, 031027 (2014).

[6] P. Hauke *et al.* Non-Abelian Gauge Fields and Topological Insulators in Shaken Optical Lattices, Phys. Rev. Lett. **109**, 145301 (2012).

[7] K. Fang, Z. Yu, and S. Fan, Realizing effective magnetic field for photons by controlling the phase of dynamic modulation, Nat. Photon. **6**, 782 (2012).

[8] P. Ponte, Z. Papić, F. Huveneers, and D. A. Abanin, Many-Body Localization in Periodically Driven Systems, Phys. Rev. Lett. **114**, 140401 (2015).

[9] M. Bukov, M. Heyl, D. A. Huse, and A. Polkovnikov, Heating and many-body resonances in a periodically driven two-band system, Phys. Rev. B **93**, 155132 (2016).

[10] Y. Liao and M. S. Foster, Spectroscopic probes of isolated nonequilibrium quantum matter: Quantum quenches, Floquet states, and distribution functions, Phys. Rev. A **92**, 053620 (2015).

[11] L. D'Alessio and A. Polkovnikov, Many-body energy localization transition in periodically driven systems, Ann. Phys. (NY) **333**, 19 (2013).

[12] M. Bukov, L. D'Alessio, and A. Polkovnikov, Universal high-frequency behavior of periodically driven systems: from dynamical stabilization to Floquet engineering, Adv. Phys. **64**, 139 (2015).

[13] L. Viola and S. Lloyd, Dynamical suppression of decoherence in two-state quantum systems, Phys. Rev. A **58**, 2733 (1998).

[14] M. Ban, Photon-echo technique for reducing the decoherence of a quantum bit, J. Mod. Opt. **45**, 2315 (1998).

[15] L. Viola, E. Knill, and S. Lloyd, Dynamical Decoupling of Open Quantum Systems, Phys. Rev. Lett. **82**, 2417 (1999).

[16] P. Zanardi, Symmetrizing evolutions, Phys. Lett. A **258**, 77 (1999).

[17] E. Knill, R. Laflamme, and L. Viola, Theory of Quantum Error Correction for General Noise, Phys. Rev. Lett. **84**, 2525 (2000).

[18] K. Khodjasteh and D. A. Lidar, Fault-Tolerant Quantum Dynamical Decoupling, Phys. Rev. Lett. **95**, 180501 (2005).

[19] G. S. Uhrig, Keeping a Quantum Bit Alive by Optimized π-Pulse Sequences, Phys. Rev. Lett. **98**, 100504 (2007); **106**, 129901(E) (2011).

[20] K. Khodjasteh and L. Viola, Dynamically Error-Corrected Gates for Universal Quantum Computation, Phys. Rev. Lett. **102**, 080501 (2009).

[21] R. Blatt and C. F. Roos, Quantum simulations with trapped ions, Nat. Phys. **8**, 277 (2012).

[22] M. Grifoni and P. Hänggi, Driven quantum tunneling, Phys. Rep. **304**, 229 (1998).

[23] W. Boyes, *Instrumentation Reference Book* (Butterworth-Heinemann, New York, 2009).

[24] M. H. Fizeau, Sur une expérience relative à la vitesse de propagation de la lumiére, Comptes Rendus **39**, 90 (1849).

[25] V.-F. Duma, M. F. Nicolov, and M. Kiss, Optical choppers: Modulators and attenuators, in *Proceedings of SPIE 7469, ROMOPTO 2009, Ninth Conference on Optics: Micro- to Nanophotonics*, Vol. II (SPIE, Bellingham, WA, 2010), p. 74690V.

[26] P. Kolchin, C. Belthangady, S. Du, G. Y. Yin, and S. E. Harris, Electro-Optic Modulation of Single Photons, Phys. Rev. Lett. **101**, 103601 (2008).

[27] I.-C. Hoi, C. M. Wilson, G. Johansson, T. Palomaki, B. Peropadre, and P. Delsing, Demonstration of a Single-Photon Router in the Microwave Regime, Phys. Rev. Lett. **107**, 073601 (2011).

[28] L. Mandel and E. Wolf, *Optical Coherence and Quantum Optics* (Cambridge University Press, Cambridge, England, 1995).

[29] D. Bouwmeester, A. K. Ekert, and A. Zeilinger, *The Physics of Quantum Information* (Springer, Berlin, 2000).

[30] R. A. Pinto, A. N. Korotkov, M. R. Geller, V. S. Shumeiko, and J. M. Martinis, Analysis of a tunable coupler for superconducting phase qubits, Phys. Rev. B **82**, 104522 (2010).

[31] R. C. Bialczak, M. Ansmann, M. Hofheinz, M. Lenander, E. Lucero, M. Neeley, A. D. O'Connell, D. Sank, H. Wang, M. Weides, J. Wenner, T. Yamamoto, A. N. Cleland, and J. M. Martinis, Fast Tunable Coupler for Superconducting Qubits, Phys. Rev. Lett. **106**, 060501 (2011).

[32] Y. Yin, Y. Chen, D. Sank, P. J. J. O'Malley, T. C. White, R. Barends, J. Kelly, E. Lucero, M. Mariantoni, A. Megrant, C. Neill, A. Vainsencher, J. Wenner, A. N. Korotkov, A. N. Cleland, and J. M. Martinis, Catch and Release of Microwave Photon States, Phys. Rev. Lett. **110**, 107001 (2013).

[33] M. Pierrea, I.-M. Svensson, S. R. Sathyamoorthy, G. Johansson, and P. Delsing, Storage and on-demand release of microwaves using superconducting resonators with tunable coupling, Appl. Phys. Lett. **104**, 232604 (2014).

[34] R. Harris, A. J. Berkley, M. W. Johnson, P. Bunyk, S. Govorkov, M. C. Thom, S. Uchaikin, A. B. Wilson, J. Chung, E. Holtham, J. D. Biamonte, A. Yu. Smirnov, M. H. S. Amin, and A. M. van den Brink, Sign- and Magnitude-Tunable Coupler for Superconducting Flux Qubits, Phys. Rev. Lett. **98**, 177001 (2007).

[35] A. O. Niskanen, K. Harrabi, F. Yoshihara, Y. Nakamura, S. Lloyd, and J. S. Tsai, Quantum coherent tunable coupling of superconducting qubits, Science **316**, 723 (2007).

[36] S. H. W. van der Ploeg, A. Izmalkov, A. Maassen van den Brink, U. Hübner, M. Grajcar, E. Il'ichev, H.-G. Meyer, and A. M. Zagoskin, Controllable Coupling of Superconducting Flux Qubits, Phys. Rev. Lett. **98**, 057004 (2007).

[37] T. Hime, P. A. Reichardt, B. L. T. Plourde, T. L. Robertson, C.-E. Wu, A. V. Ustinov, and J. Clarke, Solid-state qubits with current-controlled coupling, Science **314**, 1427 (2006).

[38] M. S. Allman, F. Altomare, J. D. Whittaker, K. Cicak, D. Li, A. Sirois, J. Strong, J. D. Teufel, and R. W. Simmonds, rf-SQUID-Mediated Coherent Tunable Coupling between a Superconducting Phase Qubit and a Lumped-Element Resonator, Phys. Rev. Lett. **104**, 177004 (2010).

[39] S. J. Srinivasan, A. J. Hoffman, J. M. Gambetta, and A. A. Houck, Tunable Coupling in Circuit Quantum

Electrodynamics Using a Superconducting Charge Qubit with a V-Shaped Energy Level Diagram, Phys. Rev. Lett. **106**, 083601 (2011).

[40] Y. Chen, C. Neill, P. Roushan, N. Leung, M. Fang, R. Barends, J. Kelly, B. Campbell, Z. Chen, B. Chiaro, A. Dunsworth, E. Jeffrey, A. Megrant, J. Y. Mutus, P. J. J. O'Malley, C. M. Quintana, D. Sank, A. Vainsencher, J. Wenner, T. C. White, M. R. Geller, A. N. Cleland, and J. M. Martinis, Qubit Architecture with High Coherence and Fast Tunable Coupling, Phys. Rev. Lett. **113**, 220502 (2014).

[41] U. Peskin and N. Moiseyev, Time-dependent scattering theory for time-periodic Hamiltonians: Formulation and complex-scaling calculations of above-threshold-ionization spectra, Phys. Rev. A **49**, 3712 (1994).

[42] W. Li and L. E. Reichl, Floquet scattering through a time-periodic potential, Phys. Rev. B **60**, 15732 (1999).

[43] A. Emmanouilidou and L. E. Reichl, Floquet scattering and classical-quantum correspondence in strong time-periodic fields, Phys. Rev. A **65**, 033405 (2002).

[44] M. V. Moskalets, *Scattering Matrix Approach to Non-Stationary Quantum Transport* (Imperial College Press, London, 2011).

[45] M. Moskalets, Two-electron state from the Floquet scattering matrix perspective, Phys. Rev. B **89**, 045402 (2014).

[46] T. Bilitewski and N. R. Cooper, Scattering theory for Floquet-Bloch states, Phys. Rev. A **91**, 033601 (2015).

[47] M. Pletyukhov and V. Gritsev, Scattering of massless particles in one-dimensional chiral channel, New J. Phys. **12**, 095028 (2012).